
Sparse Modular Activation for Efficient Sequence Modeling

Liliang Ren^{1*} Yang Liu² Shuohang Wang² Yichong Xu[†]
 Chenguang Zhu² Chengxiang Zhai¹

¹University of Illinois at Urbana-Champaign ²Microsoft
 {liliang3,czhai}@illinois.edu
 {yaliu10,shuowa,chezhu}@microsoft.com
 xuy11@gmail.com

Abstract

Linear State Space Models (SSMs) have demonstrated strong performance in a variety of sequence modeling tasks due to their efficient encoding of the recurrent structure. However, in more comprehensive tasks like language modeling and machine translation, self-attention-based models still outperform SSMs. Hybrid models employing both SSM and self-attention generally show promising performance, but current approaches apply attention modules statically and uniformly to all elements in the input sequences, leading to sub-optimal quality-efficiency trade-offs. In this work, we introduce *Sparse Modular Activation* (SMA), a general mechanism enabling neural networks to sparsely and dynamically activate sub-modules for sequence elements in a differentiable manner. Through allowing each element to skip non-activated sub-modules, SMA reduces computation and memory consumption at both training and inference stages of sequence modeling. As a specific instantiation of SMA, we design a novel neural architecture, *SeqBoat*, which employs SMA to sparsely activate a Gated Attention Unit (GAU) based on the state representations learned from an SSM. By constraining the GAU to only conduct local attention on the activated inputs, *SeqBoat* can achieve linear inference complexity with theoretically infinite attention span, and provide substantially better quality-efficiency trade-off than the chunking-based models. With experiments on a wide range of tasks, including language modeling, speech classification and long-range arena, *SeqBoat* brings new state-of-the-art results among hybrid models with linear complexity and reveals the amount of attention needed for each task through the learned sparse activation patterns.¹

1 Introduction

Recent advance on efficient sequence modeling with State Space Models (SSMs) [GGR21; GDE⁺20; GGGR22; GB22; SWL23] has shown impressive performance for a wide range of tasks across modalities, such as text classification, image recognition and speech recognition. SSMs, as first-order linear models, defined by a set of input, output, and state variables connected by first-order differential equations, can efficiently capture the recurrent structure in sequential data with carefully designed state matrices and the application of convolutional parallelism [GGR21]. However, they still significantly underperform the second-order self-attention [BCB14; VSP⁺17] based model in both language modeling and machine translation [VPSP23] tasks. A recent work [FDS⁺23] reveals that

*Work partially done during internship at Microsoft.

[†]Work done at Microsoft.

¹Our code is publicly available at <https://github.com/renll/SeqBoat>.

this is due to its deficiency of modeling pairwise comparison between the input tokens, and shows that the augmentation of an additional shifted SSM layer can improve SSM’s associative recalling ability. Furthermore, better quality-efficiency trade-off can be achieved by directly introducing extra self-attention modules to form a hybrid model (e.g. MEGA [MZK⁺23] and Hybrid H3 [FDS⁺23]) that utilizes both the first and the second order inductive biases, *i.e.*, SSM and self-attention. However, the current hybrid models apply the attention modules statically and uniformly to each of the input token regardless the property of the task itself. This can lead to sub-optimal quality-efficiency trade-offs since not all input tokens require second-order modeling and this computation need can vary substantially depending on both its context and the task difficulty.

In this paper, we aim to answer the following research questions for efficiently combining attention with SSMs: 1) Can neural networks learn to activate their attention modules dynamically to achieve better quality-efficiency trade-off? 2) How much extra attention is needed for the SSMs on a task-by-task basis? To answer these questions, we develop a new general mechanism, *Sparse Modular Activation (SMA)*, that allows a neural network to sparsely and dynamically activate its sub-modules for each of the input token in a fully differentiable manner. Specifically, we assume a neural sequence model can be composed of multiple heterogeneous sub-modules. For the input sequence, a latent configurator sparsely maps tokens to multiple compressed sequences corresponding to sub-modules. Each sub-module is then only applied on its mapped shorter sequence. Compared with activating all sub-modules on the whole input, Sparse Modular Activation can reduce both computation and memory consumption.

Efficient learning of dynamic sparsity is notoriously difficult under the constraint of the current parallel hardware [LQC⁺22; GZYE20; XM22]. To enable the practical efficiency gains from our module-level sparsity, we provide a simple yet efficient parallel implementation of SMA without any custom fused GPU kernels. Specifically, when compressing a batch of sequences in SMA, our implementation conducts both token selection and the sequence re-padding simultaneously using a single *scatter* operation that is widely optimized and present in modern deep learning frameworks.

As a specific application of the proposed SMA, we construct a novel neural architecture, *SeqBoat*, to sparsely activate a Gated Attention Unit (GAU) [HDLL22] based on the token representation learned from an SSM. Both the GAU and the SSM representations are then aggregated through simple addition and activation to form a layer-level representation. Multiple SeqBoat layers with the same hidden size are stacked sequentially to form a full neural model. Inspired by the working memory mechanism [AS68] used in human cognition, we can further restrict the GAU to only apply local attention on the compressed sequence, which allows our model to have linear sequence inference complexity but theoretically infinite attention span.

We conduct comprehensive experiments to show that SeqBoat has significantly better quality-efficiency trade-off than state-of-the-art hybrid models on a wide range of tasks, including Long Range Arena (LRA) [TDA⁺20], speech classification [War18] and language modeling. Thanks to the intrinsic modular sparsity brought by SMA, we reveal the amount of attention needed for each of the tasks through analyzing the sparse activation patterns learned by our SeqBoat model. We further demonstrate that our working memory mechanism provides substantially better computation-accuracy trade-off than the chunking based models, and analyze the relationship between the working memory size and the effective attention span on various long-range sequence modeling tasks.

2 Background

To motivate and clarify our proposed techniques, we first present a mathematical formulation of our Sparse Modular Activation mechanism and show how it encompasses and generalizes previous attempts that aimed for module-level dynamic sparsity. We begin by reviewing how the standard sequence modeling is formalized to establish the common ground for our discussion.

2.1 Time-Invariant Sequence Modeling

Given a discrete sequence, $\mathbf{x} = \{x_1, \dots, x_n\} \in \mathbb{R}^n$, consisting of n tokens, a time-invariant sequence model P_θ is optimized to maximize the likelihood of the observed sequences by factorizing them as

follows:

$$\max_{\theta} P_{\theta}(\mathbf{x}) = \prod_{t=1}^n P(x_t | \mathbf{x}_{<t}, \theta),$$

where $\mathbf{x}_{<t} = \{x_1, \dots, x_{t-1}\}$ is the sequence history at time step t , and the parameter θ is independent of the time step t . This formulation implies that the full model parameters θ and the full history $\mathbf{x}_{<t}$ are both essential for the conditional prediction of each token x_t . However, one potential issue is as the prediction difficulty of each token may differ depending on the context and the position, this static model P_{θ} can lead to sub-optimal accuracy-efficiency trade-off by wasting computation on either unimportant context [SJP⁺21] or easy-to-predict tokens [Gra16].

3 Learning Sparse Modular Activation

To provide a more efficient sequence modeling, we propose to formulate sequence modeling as a problem of finding an optimal time-variant model that can dynamically select a subset of sub-modules from a pre-defined module space for each time step.

3.1 Time-Variant Sequence Modeling

Formally, a time-variant sequence model is defined on a compact function space $\mathcal{F} : \mathcal{X}^c \mapsto [0, 1]^V$, where V is the size of the vocabulary and $\mathbf{x}_t^c \subseteq \mathbf{x}_{<t}$, $\mathbf{x}_t^c \in \mathcal{X}^c \subseteq \mathcal{X} \subseteq \mathbb{R}^n$, is a subset of the sequence history $\mathbf{x}_{<t}$. Then for each of the token prediction at the time step t , the model learns to apply a function $f_t \in \mathcal{F}$ with the parameters θ_t that maximizes the sequence probability, *i.e.*,

$$\max_{f_t, \theta_t, \mathbf{x}_t^c} P_{\mathcal{F}}(\mathbf{x}) = \prod_{t=1}^n P_{f_t}(x_t | \mathbf{x}_t^c, \theta_t) \quad \text{s.t.} \quad \mathbf{x}_t^c \subseteq \mathbf{x}_{<t} \quad (1)$$

This formulation generalizes the previous works in pursuing a dynamic and sparse model for sequence modeling, where the connections are further explained in Section 6. In this work, we assume the function space \mathcal{F} is chain-structured, *i.e.*, $\mathcal{F} = \mathcal{H} \circ \mathcal{L}_N \circ \dots \circ \mathcal{L}_1 \circ \mathcal{E}$, where $\mathcal{H} : \mathbb{R}^{n \times d_m} \mapsto [0, 1]^V$ is the classification function, $\mathcal{E} : \mathbb{R}^n \mapsto \mathbb{R}^{n \times d_m}$ is the embedding function, N is the number of intermediate layers, d_m is the model size and $\mathcal{L} : \mathbb{R}^{n \times d_m} \mapsto \mathbb{R}^{n \times d_m}$ is the function space of the intermediate mappings. We further assume that \mathcal{L} is the spanning set of a finite number of the function f_i^l with its parameters θ_i^l , *i.e.*, $\mathcal{L} = \text{span}\{f_1^l, \dots, f_M^l\}$, where M is the number of pre-defined functions. These assumptions justify the design of our Sparse Modular Activation mechanism, which is further explained in the following section.

3.2 Sparse Modular Activation

Sparse Modular Activation (SMA) introduces a latent configurator at each time step t and each layer of a neural sequence model. The configurator produces a binary decision vector $\mathbf{a}_t \in \{0, 1\}^M$ to only activate those functions f_i^l that have the decision value $a_t^i = 1$. Only the activated function will be applied to process the input representations and return the outputs. These outputs are then aggregated with a linear combination to generate the final vector, \mathbf{y}_t , of the layer. To enable end-to-end differentiability, we also require the latent configurator to output the confidence probability of its decisions, $\mathbf{c}_t \in [0, 1]^M$, and respectively scale the output from the activated function with its confidence values c_t^i . The function space of a layer equipped with SMA can be described as follow,

$$\mathcal{L}_{\text{SMA}} = \left\{ \sum_{i \in I} \zeta_i c_t^i f_i^l \mid \forall \zeta_i \in \mathbb{R}, I = \{i \mid a_t^i = 1, 1 \leq i \leq M\} \right\}$$

From this equation, we can see that the original function space \mathcal{L} is recovered, *i.e.*, $\mathcal{L}_{\text{SMA}} = \mathcal{L}$, if all the functions are activated, and the model can adaptively select any subset of the function space \mathcal{L} through controlling the binary decision vector \mathbf{a}_t . During sequential inference stage, for each function that requires the contextual information, we keep a record of its activated input representation across the time steps to form a memory $\mathbf{H}_t^c \subseteq \mathbf{H}_{<t}^c \in \mathbb{R}^{n \times d_m}$ (where $\mathbf{H}_{<t}$ is the input sequence history), so that each function can recall its contextual memory for each of the decoding step. During parallel training stage, the activated input representations for each function (or module) are sparsely

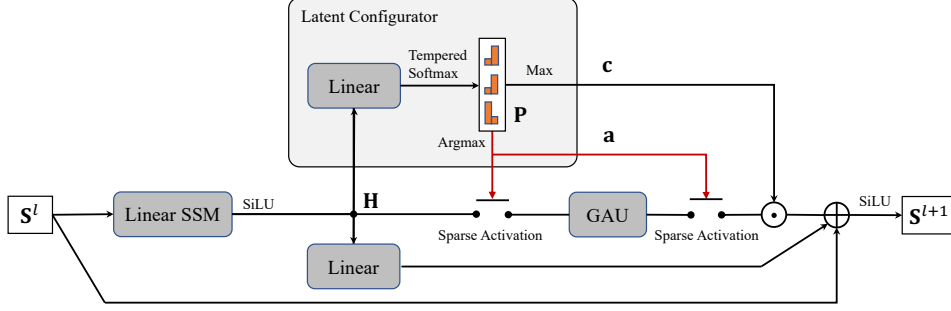


Figure 2: The proposed SeqBoat layer. The black lines indicate that the gradients can be back-propagated and the red lines stand for gradients blocking. \odot means the element-wise multiplication, and \oplus is the point-wise addition. The *max*, *argmax* and *softmax* operators are all applied to the projected dimension after the linear layer in the latent configurator block. The sparse activation operators are respectively instantiated as *compress* and *extract* operators for parallel processing.

selected to compose the compressed sequence \mathbf{H}^c for the module to conduct parallel processing. The returned representations are then extracted to its original position in a new sequence whose inactivated positions are filled with zero vectors. We illustrate this parallel implementation in Figure 1 for better understanding. The *compress* operator sparsely maps the activated inputs to form a shorter sequence for the corresponding module to process, while the *extract* operator maps the outputs from the modules to their positions in the original sentence. The Pytorch-like [PGM⁺19] code snippets are provided in the Appendix A.1 for both compression and the extraction operator with an efficient support of batched sequences.

The general framework of SMA can be instantiated in many different ways. In this paper, we explore a specific application of SMA, in which the following two types of functions in the function space \mathcal{L} are considered: (1) a linear State Space Model (SSM) [GGGR22; MZK⁺23] that efficiently captures the recurrent sequential structure, and (2) a Gated Attention Unit (GAU) [HDLL22] that performs second-order pairwise comparisons between the sequence elements. Both of the functions are instantiated as the neural modules with learnable parameters that are independent across layers. We also keep the SSM as an always-activated module and only apply SMA to the GAU. This is because for long sequence modeling, the main computation and memory bottleneck comes from the second-order self-attention and the gating operations inside the GAU module. We modularize the combination of SSM, GAU and SMA as a neural layer, which we call a SeqBoat layer. Its details are further explained in the next section.

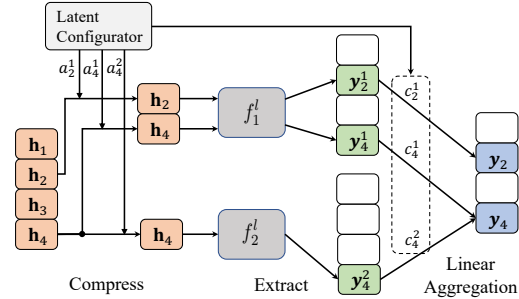


Figure 1: The proposed parallel implementation of the Sparse Modular Activation (SMA) mechanism. In this example, we have two modules f_1^l, f_2^l and an input sequence $\mathbf{H} = \{h_1, \dots, h_4\}$. We assume only a_2^1, a_4^1, a_4^2 have values equal to one. The white block means a zero vector. The compressed sequences for modules f_1^l and f_2^l are $\mathbf{H}_1^c = \{h_2, h_4\}$ and $\mathbf{H}_2^c = \{h_4\}$ respectively.

3.3 Model Architecture

Figure 2 illustrates the proposed architecture for our SeqBoat layer. Given an input sequence representation $\mathbf{S}^l \in \mathbb{R}^{n \times d_m}$ for the l -th layer, where n is the length of the sequence and d_m is the hidden size, we first apply a linear time-invariant State Space Model (SSM) [GGR21] over the sequence followed by a SiLU activation [EUD17] to obtain the state representations $\mathbf{H} \in \mathbb{R}^{n \times d_m}$,

$$\begin{aligned} \text{SSM}(\mathbf{S}^l) &= \mathbf{K} * \mathbf{S}^l + \mathbf{D} \odot \mathbf{S}^l \\ \mathbf{H} &= \text{SiLU}(\text{SSM}(\mathbf{S}^l)) \end{aligned}$$

where $*$ is a convolution operator which is efficiently implemented using FFTs [GGR21], \odot indicates the element-wise multiplication, $\mathbf{D} \in \mathbb{R}^{1 \times d_m}$ is the learnable parameters, and $\mathbf{K} \in \mathbb{R}^n$ is the SSM convolution kernel. In this work, we use the Multi-head Exponential Moving Average (MH-EMA) proposed by MEGA [MZK⁺23] for the kernel parameterization. Note that our work is perpendicular to the design of the SSM kernel as long as the kernel can provide an efficient computation of the recurrent state representation. It is possible that using a more advanced SSM such as Liquid-S4 [HLW⁺22] or S5 [SWL23] can lead to better performance, but we keep using MH-EMA for a fair comparison with MEGA. Given the state representation $\mathbf{H} \in \mathbb{R}^{n \times d_m}$, a latent configurator with one linear layer is applied to obtain the decision vector $\mathbf{a} \in \mathbb{R}^n$ and the confidence probability vector $\mathbf{c} \in \mathbb{R}^n$ with the Tempered Softmax, *i.e.*,

$$\mathbf{p}_i = \frac{e^{(\mathbf{H}\mathbf{w}_i + b_i)/\tau}}{e^{(\mathbf{H}\mathbf{w}_0 + b_0)/\tau} + e^{(\mathbf{H}\mathbf{w}_1 + b_1)/\tau}} \quad \text{for } i \in \{0, 1\}$$

$$\mathbf{a} = \arg \max_i \mathbf{p}_i, \quad \mathbf{c} = \max_i \mathbf{p}_i$$

where $\mathbf{w}_0, \mathbf{w}_1 \in \mathbb{R}^{d_m}, b_0, b_1 \in \mathbb{R}$ are learnable parameters, $\tau \in \mathbb{R}_{>0}$ is a learnable temperature parameter which is initialized as $\alpha\sqrt{d_m}$ (where α is a hyperparameter denoted as the initial temperature scale). Previous works [RSVG20a; GLL⁺22; FZS22; RZW⁺22] often seek applying auxiliary losses to regularize the exploration and the exploitation of the latent decisions. However, in this work, we don't apply any auxiliary losses and empirically observe that solely using Tempered Softmax works well for SMA. To provide an explanation of this phenomenon, we prove that the implicit regularization [BD20] of gradient decent will encourage the exploration of the latent decisions if the Softmax function with learnable temperature (*i.e.* Tempered Softmax) is used for decision confidence calculation. The details of the theorem and the proof are provided in Appendix B.

Based on the decision values \mathbf{a} , a Gated Attention Unit (GAU) is activated and applied on the compressed sequence \mathbf{H}^c resulted from the compress operator as previously described in Section 3.2,

$$\begin{aligned} \mathbf{H}^c &= \text{Compress}(\mathbf{H}, \mathbf{a}) && \in \mathbb{R}^{r \times d_m} \\ \mathbf{Y}^c &= \text{GAU}(\mathbf{H}^c) && \in \mathbb{R}^{r \times d_m} \\ \mathbf{Y} &= \text{Extract}(\mathbf{Y}^c, \mathbf{a}) && \in \mathbb{R}^{n \times d_m} \end{aligned}$$

where $r = \sum_{t=1}^n a_t$ is the total number of the time steps when the GAU module is activated. We use Squared ReLU [SML⁺21] for the attention function on the image tasks and Softmax for the text related tasks. Note that the relative position encoding inside the GAU is calculated based on the token positions in the original sentence \mathbf{H} instead of the compressed sequence \mathbf{H}^c . The detailed implementation of GAU is shown in Appendix A.2. With the extracted output $\mathbf{Y} \in \mathbb{R}^{n \times d_m}$, the final layer output is computed with a linear aggregation followed by a non-linear activation, *i.e.*,

$$\mathbf{S}^{l+1} = \text{SiLU}(\mathbf{c} \odot \mathbf{Y} + \mathbf{HW} + \mathbf{b} + \mathbf{S}^l)$$

where $\mathbf{W} \in \mathbb{R}^{d_m \times d_m}, \mathbf{b} \in \mathbb{R}^{d_m}$ are the learnable parameters. We also add a normalization layer either before the Linear SSM (*i.e.*, Pre-Norm) in the residual branch or after the final layer output \mathbf{S}^{l+1} (*i.e.*, Post-Norm) to stabilize the training process. The SeqBoat model is then constructed as stacking N number of SeqBoat layers of the same hidden size d_m with the task specific embedding and classification layers .

Working Memory Mechanism The computation complexity of our model is dynamically dependent on the activation probability of the GAU module $p = r/n = \sum_{t=1}^n a_t/n$ for each of the SeqBoat layer. This means that the computation complexity is $O(r^2 + n \log(n))$ for parallel training and $O(r^2 + n)$ for auto-regressive decoding. While it is possible that the number of the GAU-activated time steps is far smaller than the length of the full sequence for a trained model, a random initialized SeqBoat model will still activate the GAU module for $n/2$ number of times on average, leading to a non-ideal $O(n^2)$ training complexity at the early stage of training. To solve this problem, we introduce local attention [AOA⁺20] with a sliding window of size $w \ll n$ on the compressed sequence \mathbf{H}^c during the parallel training stage. This approach is equivalent to keep a First-In-First-Out (FIFO) memory with size w of the compressed sequence history for auto-regressive decoding, and in this case the FIFO memory can be understand as a working memory [AS68] for the GAU module. With this mechanism, SeqBoat reduces the training complexity to $O(rw + n \log(n))$ and the inference

complexity to $O(rw+n)$, while maintaining the ability of attending to the key tokens whose distances from the query are longer than the working memory size w . This is because the elapsed time steps between two GAU activations is generally not bounded by the size of the working memory.

4 Experiments and Results

We evaluate the SeqBoat model on three representative long-range sequence modeling benchmarks across image, text and speech modalities to have a comprehensive understanding of its capacity. The implementation details of our model for each of the tasks are presented in Appendix A.

Besides model performance on task metrics, we also report training speed and memory consumption as the efficiency of each model. Since the dynamic sparsity of SeqBoat will affect both the speed and the memory consumption throughout the training process, we measure its training speed up as the average per step wall time across the full training stage, and the memory consumption as the average per step GPU memory allocation.

4.1 Baseline Models

We compare our proposed SeqBoat model with multiple strong baseline models besides the Transformer [VSP⁺17] and its variant Transformer-XL [DYY⁺19].

S4 [GGR21] is a linear State Space Model (SSM) that efficiently captures the recurrent structure in sequential data. It employs a new parameterization for the state space model, enabling efficient and principled modeling of long-range dependencies. S4D-LegS [GGGR22] is a simpler variant of S4 that uses a diagonal state matrix.

MEGA [MZK⁺23] is a hybrid model that combines a gated self-attention mechanism with a Multi-head Exponential Moving Average (MH-EMA) parameterized SSM. It aims to achieve a better quality-efficiency trade-off by utilizing both the first and second-order inductive biases from SSM and self-attention. MH-EMA can be considered as a simpler variant of S4 that is similar to S4D.

H3 [FDS⁺23] introduces a hybrid SSM layer that stacks a diagonal SSM and a shifted SSM to model the comparisons between the elements in a sequence. It also provides a hybrid model that includes extra self-attention layers for better language modeling performance.

S5 [SWL23] is the state-of-the-art SSM model that improves over S4 with multi-input multi-output and time-domain processing. It leverages the parallel scan operator in JAX [BFH⁺18] for an efficient implementation of recurrence unrolling.

Liquid-S4 [SWL23] extends over S4 through allowing the state transition to be input-dependent. The proposed approach can be cast back to the convolutional framework and re-use the Cauchy kernel for efficient computation.

Reformer [KKL20] is a memory-efficient variant of the Transformer that uses locality-sensitive hashing (LSH) to perform approximate nearest neighbor search for attention computation.

Performer and Linformer are two efficient variants of the Transformer model. The Performer [CLD⁺20] uses the Fast Attention via positive Orthogonal Random features algorithm to approximate the self-attention mechanism, reducing the computational complexity. The Linformer [WLK⁺20] employs low-rank approximations to project the self-attention mechanism into a lower-dimensional space, resulting in a more efficient system.

Luna [MKW⁺21] is a linear unified nested attention mechanism that approximates Softmax attention with two nested linear attention functions, resulting in linear time and space complexity.

4.2 Long Sequence Modeling

We first evaluate SeqBoat and SeqBoat-full, a variant of SeqBoat conducting the full attention over the compressed sequence without the working memory mechanism, on the Long Range Arena (LRA) benchmark [TDA⁺20]. LRA is designed to test the ability of neural models to capture long-range dependencies in various modalities with the following six tasks: ListOps [NB18], text classification (Text; [MDP⁺11]), document retrieval (Retrieval; [RMQAJ13]), image classification (Image; [KH⁺09]), Pathfinder [LKV⁺18] and its longer-range variant Path-X.

Table 1: Test accuracy on the LRA benchmark. We report the relative training speed up and memory reductions on the Text task with 4,096 sequence length. * indicates a hybrid model. “Retr.” and “Path.” are the abbreviations of Retrieval and the Pathfinder tasks respectively. Best results of linear inference complexity models are in bold, second best are underlined.

| Models | ListOps | Text | Retr. | Image | Path. | Path-X | Avg. | Speed | Mem. |
|---|--------------|--------------|--------------|--------------|--------------|--------------|--------------|-------|-------|
| <i>Quadratic Inference Complexity</i> | | | | | | | | | |
| Transformer | 37.11 | 65.21 | 79.14 | 42.94 | 71.83 | ✗ | 59.24 | 1× | 1× |
| MEGA* | 63.14 | 90.43 | 91.25 | 90.44 | 96.01 | 97.98 | 88.21 | 2.9× | 0.31× |
| <i>Sub-quadratic Inference Complexity</i> | | | | | | | | | |
| Reformer | 37.27 | 56.10 | 53.40 | 38.07 | 68.50 | ✗ | 50.67 | 0.8× | 0.24× |
| BigBird | 36.05 | 64.02 | 59.29 | 40.83 | 74.87 | ✗ | 55.01 | 1.1× | 0.30× |
| SeqBoat-full* | 61.65 | 89.60 | 91.67 | 89.96 | 95.87 | 95.28 | 87.33 | 6.2× | 0.07× |
| <i>Linear Inference Complexity</i> | | | | | | | | | |
| Performer | 18.01 | 65.40 | 53.82 | 42.77 | 77.05 | ✗ | 51.41 | 5.7× | 0.11× |
| Linformer | 35.70 | 53.94 | 52.27 | 38.56 | 76.34 | ✗ | 51.36 | 5.5× | 0.10× |
| Luna-256 | 37.98 | 65.78 | 79.56 | 47.86 | 78.55 | ✗ | 61.95 | 4.9× | 0.16× |
| S4 | 59.10 | 86.53 | 90.94 | 88.48 | 94.01 | 96.07 | 85.86 | 4.8× | 0.14× |
| S4D-LegS | 60.47 | 86.18 | 89.46 | 88.19 | 93.06 | 91.95 | 84.89 | 6.1× | 0.14× |
| S5 | <u>62.15</u> | 89.31 | 91.40 | 88.00 | <u>95.33</u> | 98.58 | <u>87.46</u> | 6.1× | 0.14× |
| Liquid-S4 | 62.75 | 89.02 | 91.20 | <u>89.50</u> | 94.8 | 96.66 | 87.32 | 1.2× | 0.17× |
| H3* | 57.50 | 88.20 | 91.00 | 87.30 | 93.00 | 91.80 | 84.80 | 6.0× | 0.24× |
| MEGA-chunk* | 58.76 | 90.19 | 90.97 | 85.80 | 94.41 | 93.81 | 85.66 | 7.0× | 0.09× |
| SeqBoat* | 61.70 | <u>89.60</u> | <u>91.28</u> | 90.10 | 96.35 | <u>96.68</u> | 87.62 | 10.4× | 0.05× |

From Table 1, we can see that compared with other hybrid models with linear inference complexity, SeqBoat achieves the best average accuracy across all tasks, with a 10.4× speed up and a 95% memory reduction compared to the Transformer. When compared with a pure SSM-based model, S4, which has more general modeling power than the MH-EMA used in our model, SeqBoat achieves a substantially higher accuracy on average with a 2.17× speed up and a 64% memory reduction. Our model even achieves a significantly better average accuracy than state-of-the-art SSM model, S5 [SWL23], with a 0.16 absolute improvement, resulting in a new high score for models with linear inference complexity. Surprisingly, SeqBoat outperforms SeqBoat-full on Pathfinder and the Path-X tasks. This demonstrates the effectiveness of our proposed working memory mechanism to efficiently capture long-range dependencies, which is further analysed in Section 5. Since the learned module-level sparsity of our model is dynamic and task-specific, we also include the measurements for training and inference speedup and training memory allocation for all the tasks of LRA in Appendix C to provide a holistic view of the efficiency of our model.

4.3 Speech Classification

We also evaluate SeqBoat on the long-range speech classification task using the Speech Commands dataset [War18]. We follow [GGR21] to use the SC10 subset of the dataset. It is a 10-class classification task of raw speech which contains sequences of length 16k. As shown in Table 2, SeqBoat achieves competitive performance compared to the state-of-the-art S4 model and MEGA, with a 1.32× speed up and a 56% memory reduction compared to MEGA.

Table 2: Test accuracy on the Speech Commands 10-way classification task of raw audio (Input length 16,000). We also report the training speed up and the memory consumption reduction compared with MEGA.

| Model | #Param. | Acc. (↑) | Speed (↑) | Mem. (↓) |
|----------------|---------|--------------|-----------|----------|
| S4 | 300K | 97.50 | - | - |
| MEGA | 300K | 96.92 | 1.00× | 1.00× |
| SeqBoat | 293K | 97.35 | 1.32× | 0.44× |

4.4 Language Modeling

We evaluate on enwik8 [Hut06], a popular language modeling benchmark. It consists of the first 100 million bytes of the English Wikipedia and is commonly used to evaluate the performance of sequence models on long-range dependencies. We follow previous studies to use it as a character-level language modeling task with a vocabulary size of around 200. In inference, we divide the test text into segments and sequentially model each segment. We report the bits per character (BPC) metric for evaluation.

As shown in Table 3, we compare SeqBoat with Transformer-XL [DYY+19], Adaptive Span [SGBJ19], and MEGA. SeqBoat achieves the best performance among all models, with a $1.09\times$ speed up compared to MEGA. This demonstrates the effectiveness of our proposed model in capturing long-range dependencies in modeling natural language texts.

Table 3: Model performance on the enwik8 character-level language modeling task with a 8192 training sequence length. Training speed up and memory consumption reduction compared with MEGA are also reported.

| Model | #Param. | bpc (\downarrow) | Speed (\uparrow) | Mem. (\downarrow) |
|----------------|---------|----------------------|----------------------|-----------------------|
| Transformer-XL | 41M | 1.06 | - | - |
| Adaptive Span | 39M | 1.02 | - | - |
| MEGA | 39M | 1.02 | $1.00\times$ | $1.00\times$ |
| SeqBoat | 39M | 1.01 | $1.09\times$ | $1.02\times$ |

5 Analysis

In this section, we analyze experimental results of SMA from several research aspects. We also include more ablation studies of our model in Appendix D.

How much attention is needed for different sequence modeling tasks?

As shown in Figure 3, we draw the activation time of the GAU module at different layers of our SeqBoat-full models for each of the task in the LRA benchmark. We measure the mean and the standard deviation (plotted as error bars) of the activation time on 100 sequences randomly sampled from the validation set of each task. The lines seem to be truncated due to the fact that different models have different number of layers. Generally, we can see that Image (in Blue) and Pathfinder (in Green) need significantly more attentions than the text-based tasks (*i.e.*, Text, Retrieval and ListOps). Another trend we can see is that the bottom layers near the inputs need much less attention than the high level layers. We suspect that this is because the SSMs with first-order complexity is already capable to capture the low-level features while the attention modules are more demanded at higher levels for conducting more complex computations of second-order pairwise comparisons.

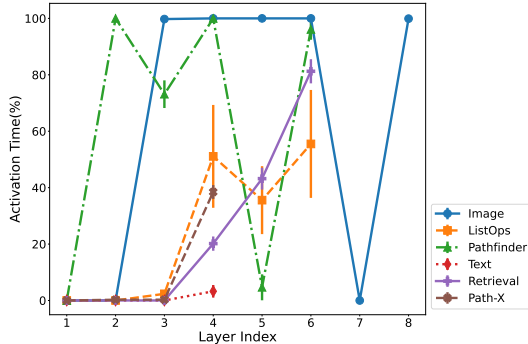


Figure 3: The activation time (with error bars) of the GAU module at different layers of the SeqBoat-full model for different tasks in the LRA benchmark. We measure the activation time as the percentage of the time steps that GAU is activated throughout the full input sequence.

How is the learned sparse modular activation distributed over the input sequence? As shown in Figure 4, we draw the confidence probabilities of the sparse modular activation for both the SeqBoat-full and the SeqBoat models on the Pathfinder task from the LRA benchmark. Generally, we can see that different input sequences has different modular activation patterns, which indicates that our modular activation is dynamically sparse. We can also see that the SeqBoat activation pattern is learned to be more structured than the SeqBoat-full, which may explain the superior performance

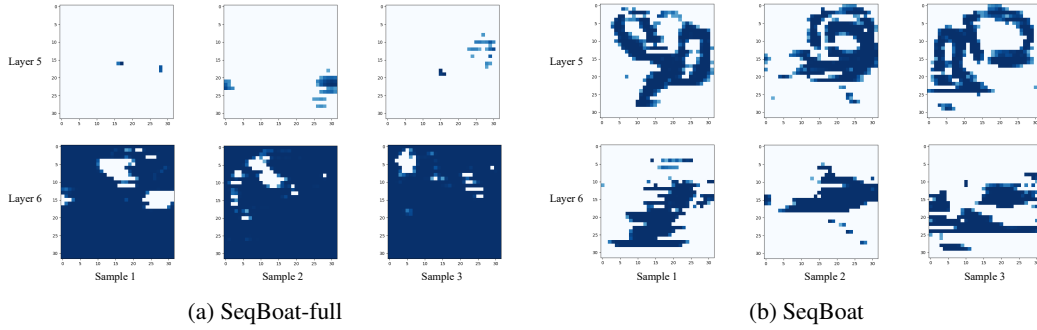


Figure 4: The confidence probabilities of the GAU modular activation at each time step for the last two layers of the SeqBoat-full and the SeqBoat model. The results are measured on three input sequences randomly sampled from the validation set of the Pathfinder task. The sequences are reshaped to 32×32 squares for better visualization. Darker the blue color, higher the confidence. The white blocks indicate the time steps when GAUs are not activated.

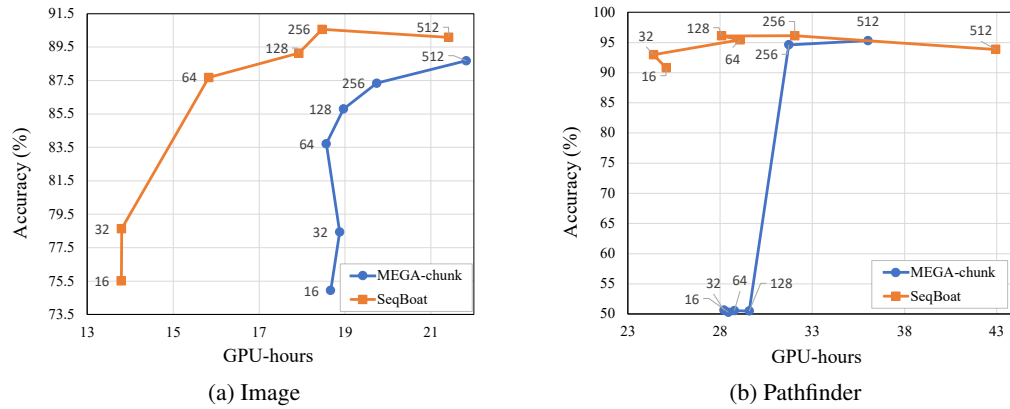


Figure 5: Training Speed v.s. Validation Accuracy trade-off on Image and Pathfinder of the LRA benchmark for different models with varying memory/chunk sizes. SeqBoat keeps a working memory of the compressed sequence, while MEGA-chunk splits the input sequence into non-overlapping sub-sequences. The memory/chunk sizes are marked along the lines. The GPU-hours for Image are measured on NVIDIA RTX A5000 GPUs, and Pathfinder on V100 GPUs with 32GB memory.

of SeqBoat over SeqBoat-full on the Pathfinder task. Another trend we can see is that different layers have their own patterns: *e.g.*, the Layer 5 of the SeqBoat model seems trying to find the curly paths in the latent representation space, while the Layer 6 seems aggregating the results from the contiguous time steps.

How does the working memory size affect the speed-quality trade-off? We compare the trade-off ability of our SeqBoat with MEGA-chunk on Image and Pathfinder tasks of the LRA benchmark, as shown in Figure 5. We draw the Pareto frontiers by respectively varying the working memory size for SeqBoat and the chunk size for MEGA-chunk from the set $\{16, 32, 64, 128, 256, 512\}$. The results are averaged with three random seeds. We can see that our models have significantly better trade-off than MEGA-chunk models for both the Image and the Pathfinder tasks. Notably, the Mega-chunk models generally fail (achieving around 50% accuracy as random guessing) on Pathfinder tasks with less than 128 chunk size, while our SeqBoat can still achieve around 90% accuracy with only a memory size of 16. This indicates the effectiveness of our working memory mechanism in capturing long term interactions.

How does the size of working memory affect the effective attention length of the GAU module? We draw Figure 6 to investigate the relationship between the working memory size and the average

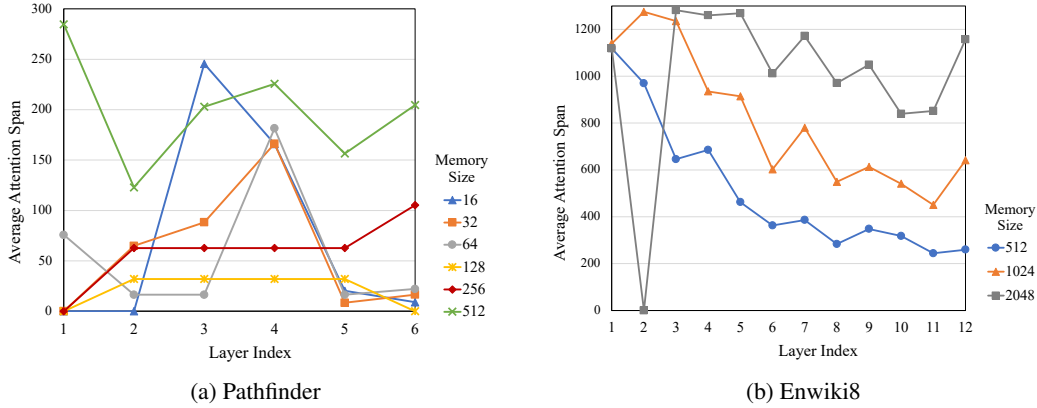


Figure 6: Working Memory Size v.s. Average Attention Span on both the Pathfinder and the Enwiki8 tasks for different SeqBoat models with different working memory sizes. A smaller layer index indicates the layer is closer to the input. For reference, the average attention span of a sliding window based local attention is the half of the window size.

effective attention length on both Pathfinder and the Enwiki8 datasets. We first measure the average attention span for each of the time step, and the results are further averaged for all the time steps in a sequence. The average attention span on Pathfinder is measured on 100 sequences randomly sampled from the validation set. The average attention span on Enwiki8 is calculated based on a sequence of length 8,192 sampled from the validation set, and each token is equipped with a minimum of 7,000 tokens context window. From the figures, we can see a general trend that the models with small working memory size (Size 16, 32 and 64 for Pathfinder, and Size 512 for Enwiki8) can have a far longer average attention span than its memory size. Notably, the layer 3 of the SeqBoat model with only 16 working memory slots surprisingly achieves an average attention span of 245 for the Pathfinder task. This partially explains the superior performance of our model over MEGA-chunk with small memory sizes and directly proves that our working memory mechanism can efficiently enable long-term interactions between the sequence elements.

6 Related Work

Various approaches pursuing module-level dynamic sparsity have been proposed in previous works.

Dynamic Routing [RSVG20b] aims to alleviate the second-order complexity of self-attention by dynamically mapping each of the token to its nearest-neighbor clusters, and only do self-attention inside the clusters. Dynamic routing can be understood as the following form when it is applied for sequence modeling,

$$\max_{\theta, \mathbf{x}_{<t}^c} P_f(\mathbf{x}) = \prod_{t=1}^n P_f(x_t | \mathbf{x}_{<t}^c, \theta)$$

where f is the Transformer architecture with self-attention layers, and it can be seen as a special case of our formulation described in Equation (1). Even though dynamic routing learns both the parameters and the corresponding context for each of the token prediction, it has a fixed architecture f that is non-adaptive for both training and the inference.

Mixture of Experts (MoE) [JJNH91; FZS22; LLX⁺20; ZLL⁺22] is designed to learn to select different parameters with the same architecture for each of the input elements. Specifically, it has the following form when applied to sequence modeling,

$$\max_{\theta_t} P_f(\mathbf{x}) = \prod_{t=1}^n P_f(x_t | \mathbf{x}_{<t}, \theta_t)$$

where the model parameter θ_t is selected from a pool of candidates at each time step t based on the input content. We can see that it is a special case of our formulation as in Section 3.1 because it has a fixed context $\mathbf{x}_{<t}$ for each of the token prediction and the model architecture is non-adaptive.

7 Conclusion

In this paper, we propose a novel general mechanism, Sparse Modular Activation (SMA), that can be used to learn sparse and adaptive activation over multiple modules in neural networks. By using State Space Models and Gated Attention Unit (GAU) as two modules for sequence modeling, we apply SMA to derive a new hybrid sequence model, SeqBoat, that has linear inference complexity through maintaining a First-In-First-Out memory of the activated input elements of the GAU, simulating human working memory. Our model shows significantly better quality-efficiency trade-offs than previous hybrid models on a wide range of sequence modeling tasks for both training and inference. Modularization of neural networks is a step toward designing biologically plausible learning systems and beneficial for scaling up a network and improving interpretability. Our work contributes a new general strategy for designing and learning module-level activation. The strong empirical performance of our models compared with other hybrid models on the sequence modeling tasks show that even with a preliminary application of SMA, we could already see substantial empirical benefits. For future work, we mainly want to explore the scaling behavior of SMA and to see if it can also provide performance gain in the context of larger models.

Acknowledgement

We would like to thank Canwen Xu, Ziyi Yang, Ruochen Xu and Azure Cognitive Services Research group members for their feedback. We also want to thank Qi Zeng and Zixuan Zhang for the early discussion of the project.

References

- [AOA⁺20] J. Ainslie, Santiago Ontañón, Chris Alberti, V. Cvicek, Zachary Kenneth Fisher, Philip Pham, Anirudh Ravula, Sumit K. Sanghai, Qifan Wang, and Li Yang. Etc: Encoding long and structured inputs in transformers. *Conference On Empirical Methods In Natural Language Processing*, 2020.
- [AS68] Richard C. Atkinson and Richard M. Shiffrin. Human memory: A proposed system and its control processes. In *The psychology of learning and motivation*, 1968.
- [BCB14] Dzmitry Bahdanau, Kyunghyun Cho, and Yoshua Bengio. Neural machine translation by jointly learning to align and translate. *International Conference On Learning Representations*, 2014.
- [BD20] D. Barrett and B. Dherin. Implicit gradient regularization. *International Conference On Learning Representations*, 2020.
- [BFH⁺18] James Bradbury, Roy Frostig, Peter Hawkins, Matthew James Johnson, Chris Leary, Dougal Maclaurin, George Necula, Adam Paszke, Jake VanderPlas, Skye Wanderman-Milne, and Qiao Zhang. JAX: composable transformations of Python+NumPy programs, 2018.
- [BZMA20] Alexei Baevski, Yuhao Zhou, Abdelrahman Mohamed, and Michael Auli. wav2vec 2.0: A framework for self-supervised learning of speech representations. *Advances in neural information processing systems*, 33:12449–12460, 2020.
- [CLD⁺20] Krzysztof Choromanski, Valerii Likhoshesterov, David Dohan, Xingyou Song, Andreea Gane, Tamas Sarlos, Peter Hawkins, Jared Davis, Afroz Mohiuddin, Lukasz Kaiser, et al. Rethinking attention with performers. *arXiv preprint arXiv:2009.14794*, 2020.
- [DMRB22] Benoit Dherin, Michael Munn, Mihaela Rosca, and David Barrett. Why neural networks find simple solutions: The many regularizers of geometric complexity. In S. Koyejo, S. Mohamed, A. Agarwal, D. Belgrave, K. Cho, and A. Oh, editors, *Advances in Neural*

- Information Processing Systems*, volume 35, pages 2333–2349. Curran Associates, Inc., 2022.
- [DYY⁺19] Zihang Dai, Zhilin Yang, Yiming Yang, Jaime Carbonell, Quoc V. Le, and Ruslan Salakhutdinov. Transformer-xl: Attentive language models beyond a fixed-length context. *ACL*, 2019.
- [EUD17] Stefan Elfving, E. Uchibe, and K. Doya. Sigmoid-weighted linear units for neural network function approximation in reinforcement learning. *Neural Networks*, 2017.
- [FDS⁺23] Daniel Y Fu, Tri Dao, Khaled Kamal Saab, Armin W Thomas, Atri Rudra, and Christopher Re. Hungry hungry hippos: Towards language modeling with state space models. In *The Eleventh International Conference on Learning Representations*, 2023.
- [FZS22] William Fedus, Barret Zoph, and Noam Shazeer. Switch transformers: Scaling to trillion parameter models with simple and efficient sparsity. *The Journal of Machine Learning Research*, 23(1):5232–5270, 2022.
- [GB22] Ankit Gupta and Jonathan Berant. Diagonal state spaces are as effective as structured state spaces. *ARXIV.ORG*, 2022.
- [GDE⁺20] Albert Gu, Tri Dao, Stefano Ermon, Atri Rudra, and Christopher Ré. Hippo: Recurrent memory with optimal polynomial projections. In H. Larochelle, M. Ranzato, R. Hadsell, M.F. Balcan, and H. Lin, editors, *Advances in Neural Information Processing Systems*, volume 33, pages 1474–1487. Curran Associates, Inc., 2020.
- [GGGR22] Albert Gu, Ankit Gupta, Karan Goel, and Christopher Ré. On the parameterization and initialization of diagonal state space models. *ARXIV.ORG*, 2022.
- [GGR21] Albert Gu, Karan Goel, and Christopher Ré. Efficiently modeling long sequences with structured state spaces. *International Conference On Learning Representations*, 2021.
- [GLL⁺22] Yue Guan, Zhengyi Li, Jingwen Leng, Zhouhan Lin, and Minyi Guo. Transkimmer: Transformer learns to layer-wise skim. In *Proceedings of the 60th Annual Meeting of the Association for Computational Linguistics (Volume 1: Long Papers)*, pages 7275–7286, Dublin, Ireland, may 2022. Association for Computational Linguistics.
- [Gra16] A. Graves. Adaptive computation time for recurrent neural networks. *ARXIV.ORG*, 2016.
- [GZYE20] Trevor Gale, M. Zaharia, C. Young, and Erich Elsen. Sparse gpu kernels for deep learning. *International Conference For High Performance Computing, Networking, Storage And Analysis*, 2020.
- [HDLL22] Weizhe Hua, Zihang Dai, Hanxiao Liu, and Quoc V. Le. Transformer quality in linear time. *International Conference On Machine Learning*, 2022.
- [HLW⁺22] Ramin Hasani, Mathias Lechner, Tsun-Hsuan Wang, Makram Chahine, Alexander Amini, and Daniela Rus. Liquid structural state-space models. *arXiv preprint arXiv:2209.12951*, 2022.
- [Hut06] Marcus Hutter. The human knowledge compression contest. <http://prize.hutter1.net/>, 2006.
- [JGP17] Eric Jang, Shixiang Gu, and Ben Poole. Categorical reparameterization with gumbel-softmax. In *5th International Conference on Learning Representations, ICLR 2017, Toulon, France, April 24-26, 2017, Conference Track Proceedings*. OpenReview.net, 2017.
- [JJNH91] Robert A. Jacobs, Michael I. Jordan, Steven J. Nowlan, and Geoffrey E. Hinton. Adaptive mixtures of local experts. *Neural Computation*, 3:79–87, 1991.
- [KH⁺09] Alex Krizhevsky, Geoffrey Hinton, et al. Learning multiple layers of features from tiny images. 2009.

- [KKL20] Nikita Kitaev, Łukasz Kaiser, and Anselm Levskaya. Reformer: The efficient transformer. *arXiv preprint arXiv:2001.04451*, 2020.
- [LKV⁺18] Drew Linsley, Junkyung Kim, Vijay Veerabadrán, Charles Windolf, and Thomas Serre. Learning long-range spatial dependencies with horizontal gated recurrent units. *Advances in neural information processing systems*, 31, 2018.
- [LLX⁺20] Dmitry Lepikhin, HyoukJoong Lee, Yuanzhong Xu, Dehao Chen, Orhan Firat, Yanping Huang, M. Krikun, Noam M. Shazeer, and Z. Chen. Gshard: Scaling giant models with conditional computation and automatic sharding. *International Conference On Learning Representations*, 2020.
- [LQC⁺22] Liu Liu, Zheng Qu, Zhaodong Chen, Fengbin Tu, Yufei Ding, and Yuan Xie. Dynamic sparse attention for scalable transformer acceleration. *IEEE Transactions on Computers*, 71:3165–3178, 2022.
- [MDP⁺11] Andrew Maas, Raymond E Daly, Peter T Pham, Dan Huang, Andrew Y Ng, and Christopher Potts. Learning word vectors for sentiment analysis. In *Proceedings of the 49th annual meeting of the association for computational linguistics: Human language technologies*, pages 142–150, 2011.
- [MKW⁺21] Xuezhe Ma, Xiang Kong, Sinong Wang, Chunting Zhou, Jonathan May, Hao Ma, and Luke Zettlemoyer. Luna: Linear unified nested attention. *Advances in Neural Information Processing Systems*, 34:2441–2453, 2021.
- [MZK⁺23] Xuezhe Ma, Chunting Zhou, Xiang Kong, Junxian He, Liangke Gui, Graham Neubig, Jonathan May, and Luke Zettlemoyer. Mega: Moving average equipped gated attention. In *The Eleventh International Conference on Learning Representations*, 2023.
- [NB18] Nikita Nangia and Samuel R Bowman. Listops: A diagnostic dataset for latent tree learning. *arXiv preprint arXiv:1804.06028*, 2018.
- [PGM⁺19] Adam Paszke, Sam Gross, Francisco Massa, Adam Lerer, James Bradbury, Gregory Chanan, Trevor Killeen, Zeming Lin, Natalia Gimelshein, Luca Antiga, et al. Pytorch: An imperative style, high-performance deep learning library. *Advances in neural information processing systems*, 32, 2019.
- [RMQAJ13] Dragomir R Radev, Pradeep Muthukrishnan, Vahed Qazvinian, and Amjad Abu-Jbara. The acl anthology network corpus. *Language Resources and Evaluation*, 47:919–944, 2013.
- [RSVG20a] Aurko Roy, M. Saffar, Ashish Vaswani, and David Grangier. Efficient content-based sparse attention with routing transformers. *International Conference On Topology, Algebra And Categories In Logic*, 2020.
- [RSVG20b] Aurko Roy, M. Saffar, Ashish Vaswani, and David Grangier. Efficient content-based sparse attention with routing transformers. *International Conference On Topology, Algebra And Categories In Logic*, 2020.
- [RZW⁺22] Liliang Ren, Zixuan Zhang, Han Wang, Clare Voss, ChengXiang Zhai, and Heng Ji. Language model pre-training with sparse latent typing. In *Proceedings of the 2022 Conference on Empirical Methods in Natural Language Processing*, pages 1480–1494, Abu Dhabi, United Arab Emirates, dec 2022. Association for Computational Linguistics.
- [SGBJ19] Sainbayar Sukhbaatar, Edouard Grave, Piotr Bojanowski, and Armand Joulin. Adaptive attention span in transformers. *arXiv preprint arXiv:1905.07799*, 2019.
- [SJP⁺21] Sainbayar Sukhbaatar, Da Ju, Spencer Poff, Stephen Roller, Arthur D. Szlam, J. Weston, and Angela Fan. Not all memories are created equal: Learning to forget by expiring. *International Conference On Machine Learning*, 2021.

- [SLK⁺18] Sihyeon Seong, Yegang Lee, Youngwook Kee, Dongyoon Han, and Junmo Kim. Towards flatter loss surface via nonmonotonic learning rate scheduling. In *Conference on Uncertainty in Artificial Intelligence*, 2018.
- [SLP⁺21] Jianlin Su, Yu Lu, Shengfeng Pan, Ahmed Murtadha, Bo Wen, and Yunfeng Liu. Roformer: Enhanced transformer with rotary position embedding. *arXiv preprint arXiv:2104.09864*, 2021.
- [SML⁺21] David R. So, Wojciech Mańke, Hanxiao Liu, Zihang Dai, Noam M. Shazeer, and Quoc V. Le. Primer: Searching for efficient transformers for language modeling. *ARXIV.ORG*, 2021.
- [SUV18] Peter Shaw, Jakob Uszkoreit, and Ashish Vaswani. Self-attention with relative position representations. *NAACL*, 2018.
- [SWL23] Jimmy T.H. Smith, Andrew Warrington, and Scott Linderman. Simplified state space layers for sequence modeling. In *The Eleventh International Conference on Learning Representations*, 2023.
- [TDA⁺20] Yi Tay, M. Dehghani, Samira Abnar, Yikang Shen, Dara Bahri, Philip Pham, J. Rao, Liu Yang, Sebastian Ruder, and Donald Metzler. Long range arena: A benchmark for efficient transformers. *International Conference On Learning Representations*, 2020.
- [VPSP23] Ali Vardasbi, Telmo Pires, Robin M. Schmidt, and Stephan Peitz. State spaces aren't enough: Machine translation needs attention. *ARXIV.ORG*, 2023.
- [VSP⁺17] Ashish Vaswani, Noam M. Shazeer, Niki Parmar, Jakob Uszkoreit, Llion Jones, Aidan N. Gomez, Lukasz Kaiser, and Illia Polosukhin. Attention is all you need. *NIPS*, 2017.
- [War18] Pete Warden. Speech commands: A dataset for limited-vocabulary speech recognition. *arXiv preprint arXiv: Arxiv-1804.03209*, 2018.
- [WLK⁺20] Sinong Wang, Belinda Z Li, Madian Khabsa, Han Fang, and Hao Ma. Linformer: Self-attention with linear complexity. *arXiv preprint arXiv:2006.04768*, 2020.
- [XM22] Canwen Xu and Julian McAuley. A survey on dynamic neural networks for natural language processing. *FINDINGS*, 2022.
- [ZLL⁺22] Yanqi Zhou, Tao Lei, Hanxiao Liu, Nan Du, Yanping Huang, Vincent Zhao, Andrew M Dai, Quoc V Le, James Laudon, et al. Mixture-of-experts with expert choice routing. *Advances in Neural Information Processing Systems*, 35:7103–7114, 2022.

A Implementation Details

A.1 Code for Compress and Extract Operators in SMA

```
def compress(q, a):
    # Args:
    #   q: Input sequences with the shape:
    #       (Batch Size, Input Sequence Length, Hidden Size)
    #   a: Binary decision values with the shape:
    #       (Batch Size, Input Sequence Length, 1)
    # Returns:
    #   Compressed sequences with the shape:
    #       (Batch Size, Compressed Sequence Length, Hidden Size)

    # Max sequence length of the compressed sequences
    max_sl = a.sum(-2).max()
    # Calculate the indices in the compressed sequence
    index_q = a * torch.cumsum(a,dim=-2)

    # Simultaneously map and pad to build the compressed sequences
    # +1 for temporarily storing non-activated elements
    shape = q.shape[:-2] + (max_sl+1,) + q.shape[-1:]
    new_q = torch.zeros(shape)
    new_q.scatter_(-2,index_q, q)
    new_q = new_q[:,1:,:] # Non-activated elements are discarded

    return new_q
```

Listing 1: Pytorch-like code snippet for the Compress operator.

```
def extract(h, a):
    # Args:
    #   h: Compressed sequences with the shape:
    #       (Batch Size, Compressed Sequence Length, Hidden Size)
    #   a: Binary decision values with the shape:
    #       (Batch Size, Input Sequence Length, 1)
    # Returns:
    #   Output sequences with zeros for non-activated positions:
    #       (Batch Size, Input Sequence Length, Hidden Size)

    # Calculate the indices in the compressed sequence
    index_q = a * torch.cumsum(a,dim=-2)
    # Pad the sequence dimension to account for non-activated positions
    h = F.pad(h, (0,0,1,0))
    h = torch.gather(h,-2,index_q.expand(-1,-1,h.shape[-1]))
    return h
```

Listing 2: Pytorch-like code snippet for the Extract operator.

A.2 Details of Gated Attention Unit

Our Gated Attention Unit (GAU) mostly follows the original implementation as [HDLL22], with slight modifications of the relative position bias. Given the compressed sequence $\mathbf{H}^c \in \mathbb{R}^{r \times d_m}$, we first compute the query, key and value sequences, $\mathbf{Q}, \mathbf{K}, \mathbf{V}$, *i.e.*,

$$\mathbf{Q} = \mathbf{w}_q \odot \mathbf{H}^c + \mathbf{b}_q \in \mathbb{R}^{r \times d_z} \quad (2)$$

$$\mathbf{K} = \mathbf{w}_k \odot \mathbf{H}^c + \mathbf{b}_k \in \mathbb{R}^{r \times d_z} \quad (3)$$

$$\mathbf{V} = \text{SiLU}(\mathbf{H}^c \mathbf{W}_v + \mathbf{b}_v) \in \mathbb{R}^{r \times d_v} \quad (4)$$

where $\mathbf{w}_q, \mathbf{w}_k, \mathbf{b}_q, \mathbf{b}_k \in \mathbb{R}^{d_z}$, $\mathbf{W}_v \in \mathbb{R}^{d_m \times d_v}$, $\mathbf{b}_v \in \mathbb{R}^{d_v}$ are the learnable parameters, \odot means the pointwise multiplication, and d_v is the expanded hidden dimension which is set as $d_v = 2d_m$ in our work. Then the attention output is calculated as,

Table 4: Hyper-parameter Settings of our SeqBoat model for the LRA benchmark and the Speech Command (SC) dataset. DP is the dropout rate, BSZ is batch size, LR is learning rate and WD is weight decay. BN, LN and SN refer to Batch Normalization, Layer Normalization and Scale Normalization.

| Task | Depth | d_m | α | d_z | d_v | Attn-FN | Norm | Pre-norm | BSZ | LR | DP | WD | Epochs |
|------------|-------|-------|----------|-------|-------|-------------------|------|----------|-----|-------|-----|-------|--------|
| ListOps | 6 | 80 | 0.3 | 64 | 160 | softmax | LN | FALSE | 64 | 0.004 | 0.1 | 0.001 | 60 |
| Text | 4 | 128 | 0.3 | 64 | 256 | softmax | SN | FALSE | 50 | 0.004 | 0.1 | 0.01 | 50 |
| Retrieval | 6 | 128 | 0.3 | 64 | 256 | softmax | SN | FALSE | 64 | 0.003 | 0.1 | 0.04 | 40 |
| Image | 8 | 160 | 0.4 | 96 | 320 | relu ² | BN | TRUE | 50 | 0.01 | 0 | 0.02 | 200 |
| Pathfinder | 6 | 128 | 1.0 | 64 | 256 | relu ² | BN | TRUE | 128 | 0.01 | 0 | 0.01 | 200 |
| Path-X | 6 | 128 | 1.0 | 64 | 256 | relu ² | BN | TRUE | 128 | 0.01 | 0 | 0.01 | 100 |
| SC-Raw | 8 | 60 | 1.0 | 30 | 120 | relu ² | BN | TRUE | 20 | 0.01 | 0 | 0.01 | 200 |

$$\mathbf{O} = f(\mathbf{Q}\mathbf{K}^T/s + \mathbf{B}_{\text{rel}})\mathbf{V} \in \mathbb{R}^{r \times d_v} \quad (5)$$

where f is the attention function, $s = r$ is the normalizing factor, $\mathbf{B}_{\text{rel}} \in \mathbb{R}^{n \times n}$ is the relative positional bias which is set as the simple relative position bias [SUV18; MZK+23] by default. We also have the choice for using RoPE [SLP+21] relative position embedding, and in this case, we don't apply relative position bias but use RoPE in its original form to transform the \mathbf{Q} and \mathbf{K} sequences. Squared ReLU is applied [SML+21] for the attention function on the image and the speech tasks and Softmax for the text related tasks. By default, the relative positions are calculated based on the token positions in the original sentence \mathbf{H} instead of the compressed sequence \mathbf{H}^c . For working memory mechanism, we conduct local attention between $\mathbf{Q}, \mathbf{K}, \mathbf{V}$ with the sliding window size (or the working memory size) w , and we set the normalizing factor $s = w$. The final output of the GAU is computed with a gating mechanism,

$$\mathbf{G} = \text{SiLU}(\mathbf{H}^c \mathbf{W}_g + \mathbf{b}_g) \in \mathbb{R}^{r \times d_v} \quad (6)$$

$$\mathbf{Y}^c = (\mathbf{G} \odot \mathbf{O})\mathbf{W}_h + \mathbf{b}_h \in \mathbb{R}^{r \times d_m} \quad (7)$$

where $\mathbf{W}_g \in \mathbb{R}^{d_m \times d_v}$, $\mathbf{W}_h \in \mathbb{R}^{d_v \times d_m}$, $\mathbf{b}_g \in \mathbb{R}^{d_v}$, $\mathbf{b}_h \in \mathbb{R}^{d_m}$ are learnable parameters.

A.3 Details of Latent Configurator with Gumbel Softmax

To produce this baseline, we apply Gumbel Softmax to the probability computation in the latent configurator described in Section 3.3. Specifically, the modified probability calculation is as follow,

$$\mathbf{p}'_i = \frac{e^{(\mathbf{H}\mathbf{w}_i + \mathbf{b}_i + G_i)/\tau'}}{e^{(\mathbf{H}\mathbf{w}_0 + \mathbf{b}_0 + G_0)/\tau'} + e^{(\mathbf{H}\mathbf{w}_1 + \mathbf{b}_1 + G_1)/\tau'}} \quad \text{for } i \in \{0, 1\}$$

where $G_i \sim \text{Gumbel}(0, 1)$ is the Gumbel noise sampled from a standard Gumbel distribution and τ' follows the following temperature annealing schedule as in the previous work [BZMA20],

$$\tau' = \max(2 \times 0.999995^T, 0.5),$$

where T is the number of training steps.

A.4 Hyper-parameter settings

We use mostly the same hyper-parameter settings as MEGA. For Long Range Arena (LRA) and Speech Command tasks, the detailed settings together with our initial temperature scale α for the latent configurator are shown in Table 4. Following S5 [SWL23], we use NLI-style fusion of encoder features for the Retrieval task of LRA. For SeqBoat model, we use a working memory size $w = 512$ for Path-X and $w = 256$ for other tasks in LRA. For Speech Command, a working memory size of 256 is used. And for language modeling tasks, we use a working memory of size 2,048. We use RoPE relative position embeddings for language modeling. For the speech command task and the Text task of LRA, the relative positions are calculated based on the positions in the compressed sequence.

B Theorem of Implicit Regularization for Latent Decision

We first give a brief introduction of the implicit regularization to provide some backgrounds. The implicit regularization of gradient decent [BD20] is a side effect caused by the discreteness of the gradient descent updates. Specifically, it has been proved that a discrete gradient update $\theta' = \theta - h\nabla_{\theta}L(\theta)$ of the parameter θ is implicitly minimizing a transformed loss, $L' = L + \frac{h}{4}\|\nabla_{\theta}L(\theta)\|^2$ where h is the learning rate and L is the training loss term. Assuming the usage of Stochastic Gradient Decent (SGD) for gradient updates, [DMRB22] have shown that the implicit gradient regularizer $\|\nabla_{\theta}L(\theta)\|^2$ will conditionally put an implicit pressure on $\|\nabla_{\theta}f_{\theta}(x)\|_F^2$ for a multi-class classification cross-entropy loss term, where $f_{\theta}(x)$ is a neural network that takes the input x and outputs the logits for classification. A Transfer Theorem [DMRB22] is further derived to characterize the conditional transfer of the implicit regularization pressure from $\|\nabla_{\theta}f_{\theta}(x)\|_F^2$ to the gradient norm $\|\nabla_x f_{\theta}(x)\|_F^2$, where $\|\cdot\|_F$ means the Frobenius norm. The transfer theorem assumes an ordinary neural architecture $f_{\theta}(x) : \mathbb{R}^d \mapsto \mathbb{R}^k$ with l layers in the following form,

$$h_i(x) = a_i(w_{h_i}h_{i-1}(x) + b_i), \quad \text{for } i = 1, 2, \dots, l,$$

where a_i is the activation function, $h_i(x)$ indicates the sub-network from the input $x \in \mathbb{R}^d$ up to the output of layer i and $h_0(x) = x$. This implies $h_l(x) = f_{\theta}(x)$.

In this work, we consider a neural architecture that has a per-layer latent configurator $p_i : \mathbb{R}^{|h_{i-1}|} \mapsto [0, 1]$, $p_i(z) = y_i(w_i z)$, that maps the hidden representation from h_{i-1} to a confidence probability of activating a submodule $q_i : \mathbb{R}^{|h_{i-1}|} \mapsto \mathbb{R}^{|h_i|}$, i.e.,

$$h_i(x) = a_i(p_i(h_{i-1}(x))q_i(h_{i-1}(x))), \quad \text{for } i = 1, 2, \dots, l,$$

where y_i is the normalizing function to produce the probability. We use a similar technique of perturbation argument [DMRB22; SLK⁺18] for proving that the implicit pressure will also transfer to the latent configurator p_i , which leads to the implicit regularization of latent activation decisions.

Theorem B.1. (Transfer Theorem for Latent Configurator). *Let $f_{\theta} : \mathbb{R}^d \rightarrow \mathbb{R}^k$ represent a deep neural network consisting of l layers, i.e., $f_{\theta}(x) = f_l \circ f_{l-1} \circ \dots \circ f_1(x)$ where $f_i(z) = a_i(p_i(z)q_i(z))$, $p_i : \mathbb{R}^{|z|} \mapsto [0, 1]$, $p_i(z) = y_i(w_i z)$ is a latent configurator, $q_i : \mathbb{R}^{|z|} \mapsto \mathbb{R}^{|h_i|}$ is a sub-module function, a_i is the activation function, y_i is the probability normalization function and w_i is a weight matrix. For $i = 1, 2, \dots, l$, we have*

$$\|\nabla_{w_i} r_i(x)\|_2^2 \frac{\|d_i(x)\|_2^2 \|\nabla_x f_{\theta}(x)\|_2^2}{\|d_i(x)\nabla_x r_i(x) + r_i(x)\nabla_x d_i(x)\|_2^2} \leq \|\nabla_{w_i} f_{\theta}(x)\|_2^2 \quad (8)$$

where $r_i(x) := p_i(h_{i-1}(x))$ and $d_i(x) := q_i(h_{i-1}(x))$, $h_i(x)$ indicates the sub-network from the input $x \in \mathbb{R}^d$ up to the output of layer i with $h_0(x) = x$ and $\|\cdot\|_2$ denotes the L2 operator norm for matrix and L2 norm for vector.

Proof. Following the above notations, we first rewrite the model function as

$$f_{w_i}(x) = g_i(r_i(x)d_i(x)),$$

where $g_i(z)$ is the remaining network of the full model $f_{\theta}(x)$ following the i -th layer. Considering a small perturbation $x + \delta x$ of the input x , there exists a corresponding perturbation $w_i + u(x)$ for the weight matrix in the latent configurator p_i so that

$$f_{w_i}(x + \delta x) = f_{w_i + u(x)}(x). \quad (9)$$

For sufficiently small δx , we can identify $r_i(x + \delta x)d_i(x + \delta x)$ with the linear approximation around x , i.e.,

$$r_i(x + \delta x)d_i(x + \delta x) = r_i(x)d_i(x) + d_i(x)\nabla_x r_i(x)\delta x + r_i(x)\nabla_x d_i(x)\delta x$$

where $\nabla_x d_i : \mathbb{R}^d \mapsto \mathbb{R}^{|h_i|}$ and $\nabla_x r_i : \mathbb{R}^d \mapsto [0, 1]$ are the total derivatives. We have

$$\begin{aligned} f_{w_i}(x + \delta x) &= g_i(r_i(x + \delta x)d_i(x + \delta x)) \\ &= g_i(r_i(x)d_i(x) + d_i(x)\nabla_x r_i(x)\delta x + r_i(x)\nabla_x d_i(x)\delta x), \end{aligned}$$

and similarly, for $r_i(x) = y_i(w_i h_{i-1}(x))$, and the perturbation $w_i \rightarrow w_i + u(\delta x)$, we can have the linear approximation $r'_i(x) = y_i((w_i + u(\delta x))h_{i-1}(x)) = r_i(x) + \nabla_{w_i} r_i(x)u(\delta x)$. This implies

$$f_{w_i+u(\delta x)}(x) = g_i(r_i(x)d_i(x) + \nabla_{w_i} r_i(x)u(\delta x)d_i(x)).$$

Therefore, substituting both sides of Equation (9) with the equations above, and we get

$$\nabla_{w_i} r_i(x)u(\delta x)d_i(x) = d_i(x)\nabla_x r_i(x)\delta x + r_i(x)\nabla_x d_i(x)\delta x.$$

Note the fact that $\nabla_{w_i} r_i(x)^T \nabla_{w_i} r_i(x) = \|\nabla_{w_i} r_i(x)\|_2^2$. This implies

$$u(\delta x) = \frac{\nabla_{w_i} r_i(x)^T (d_i(x)\nabla_x r_i(x)\delta x + r_i(x)\nabla_x d_i(x)\delta x)d_i(x)^T}{\|\nabla_{w_i} r_i(x)\|_2^2 \|d_i(x)\|_2^2}. \quad (10)$$

Defining $u(\delta x)$ as above and taking the derivative of both sides of Equation (9) with respect to δx at $\delta x = 0$, we have

$$\nabla_x f_{w_i}(x) = \nabla_{w_i} f_\theta(x) \frac{\nabla_{w_i} r_i(x)^T (d_i(x)\nabla_x r_i(x) + r_i(x)\nabla_x d_i(x))d_i(x)^T}{\|\nabla_{w_i} r_i(x)\|_2^2 \|d_i(x)\|_2^2}.$$

Applying the squared L2 operator norm $\|\cdot\|_2^2$, at both sides of the equation, we get

$$\begin{aligned} \|\nabla_x f_{w_i}(x)\|_2^2 &= \left\| \nabla_{w_i} f_\theta(x) \frac{\nabla_{w_i} r_i(x)^T (d_i(x)\nabla_x r_i(x) + r_i(x)\nabla_x d_i(x))d_i(x)^T}{\|\nabla_{w_i} r_i(x)\|_2^2 \|d_i(x)\|_2^2} \right\|_2^2 \\ &\leq \|\nabla_{w_i} f_\theta(x)\|_2^2 \frac{\|d_i(x)\nabla_x r_i(x) + r_i(x)\nabla_x d_i(x)\|_2^2}{\|\nabla_{w_i} r_i(x)\|_2^2 \|d_i(x)\|_2^2}. \end{aligned}$$

Since $\nabla_x f_{w_i}(x) = \nabla_x f_\theta(x)$, this completes the proof. \square

Remarks Considering the architecture of the latent configurator in the SeqBoat layer, *i.e.*, the activation confidence probability is calculated as

$$p_i(z) = \frac{e^{z \cdot w_i^1 / \tau_i}}{e^{z \cdot w_i^0 / \tau_i} + e^{z \cdot w_i^1 / \tau_i}},$$

then we can derive the squared L2 norms of its derivatives,

$$\begin{aligned} \|\nabla_{w_i^1} p_i(z)\|_2^2 &= \|\nabla_{w_i^0} p_i(z)\|_2^2 = (p_i(z)(1 - p_i(z))\|z\|_2 / \tau_i)^2, \\ \|\nabla_z p_i(z)\|_2^2 &= (p_i(z)(1 - p_i(z))\|w_i^0 - w_i^1\|_2 / \tau_i)^2. \end{aligned}$$

Substituting the above gradient values to Equation (8), we can see that

$$\begin{aligned} \|\nabla_{w_i} r_i(x)\|_2^2 \frac{\|d_i(x)\|_2^2 \|\nabla_x f_\theta(x)\|_2^2}{\|d_i(x)\nabla_x r_i(x) + r_i(x)\nabla_x d_i(x)\|_2^2} &\leq \|\nabla_{w_i} f_\theta(x)\|_2^2 \\ \implies \frac{\|h_{i-1}(x)\|_2^2 \|d_i(x)\|_2^2 \|\nabla_x f_\theta(x)\|_2^2}{\|d_i(x)\|_2^2 \|\nabla_x h_{i-1}(x)\|_2^2 \|w_i^0 - w_i^1\|_2^2 + \frac{\|\nabla_x d_i(x)\|_2^2 \tau_i^2}{(1 - p_i(h_{i-1}(x)))^2}} &\leq \|\nabla_{w_i} f_\theta(x)\|_2^2 \end{aligned}$$

This implies that the implicit regularization pressure will tend to maximize the temperature τ_i to increase the exploration of the latent decisions, while at the same time maximize the probability of modular activation or de-activation through maximizing $\|w_i^0 - w_i^1\|_2^2$ and $p_i(h_{i-1}(x))$ for exploiting the decisions. Therefore, there will be an implicit balancing between the exploration and the exploitation of the latent decisions, and we suspect this kind of balancing is the cause of the dynamic sparse activation patterns we observed from the experiments.

C Additional Experiments and Results

C.1 Per-task Efficiency Measures for LRA Benchmark

As shown in Table 5, we compare the efficiency of our SeqBoat-full and SeqBoat models with the Mega and its chunk variants on all six tasks of the LRA benchmark. The evaluation speed is measured as the average inference throughput of the best performing model on the validation set. All the relative efficiency measures between different models are conducted on a server with 8 NVIDIA V100 32GB GPUs under the same batch size settings for fair comparisons. We can see that our SeqBoat model is consistently and substantially more efficient than Mega, and it also has comparable efficiency with Mega-chunk but significantly better average accuracy on the LRA benchmark.

Table 5: Per-task speed up and memory allocation reduction on the LRA benchmark.

| Models (Input Length) | ListOps (2,048) | Text (4,096) | Retrieval (4,000) | Image (1,024) | Path (1,024) | Path-X (16,384) |
|--|---------------------------|------------------------|-----------------------------|-------------------------|------------------------|---------------------------|
| <i>Training Step Speed Up (↑)</i> | | | | | | |
| MEGA | 1.00× | 1.00× | 1.00× | 1.00× | 1.00× | 1.00× |
| MEGA-chunk | 2.07× | 2.42× | 2.66× | 1.39× | 1.46× | 1.36× |
| SeqBoat-full | 1.79× | 2.14× | 1.91× | 1.45× | 1.27× | 1.24× |
| SeqBoat | 2.29× | 3.73× | 1.99× | 1.49× | 1.33× | 1.30× |
| <i>Training Step Memory Allocation (↓)</i> | | | | | | |
| MEGA | 1.00× | 1.00× | 1.00× | 1.00× | 1.00× | 1.00× |
| MEGA-chunk | 0.34× | 0.29× | 0.31× | 0.75× | 0.69× | 0.82× |
| SeqBoat-full | 0.45× | 0.23× | 0.32× | 0.74× | 0.68× | 0.59× |
| SeqBoat | 0.30× | 0.15× | 0.22× | 0.68× | 0.65× | 0.89× |
| <i>Evaluation Step Speed Up (↑)</i> | | | | | | |
| MEGA | 1.00× | 1.00× | 1.00× | 1.00× | 1.00× | 1.00× |
| MEGA-chunk | 2.15× | 2.33× | 2.57× | 1.48× | 1.50× | 2.52× |
| SeqBoat-full | 1.70× | 2.47× | 1.57× | 1.52× | 1.30× | 1.95× |
| SeqBoat | 2.70× | 3.60× | 2.00× | 1.58× | 1.37× | 1.93× |

D Additional Analysis

How does different model design choices affect the performance? We do the ablation study of our model on the Image and ListOps tasks of the LRA benchmark, as in Table 6. “Always Activated” means that we don’t use SMA and always activate GAU for conducting second-order self-attention. We can see that although the validation accuracy is slightly improved on both Image and Listops, the training efficiency drops significantly. We also explore different parameterization of the convolution kernel for the linear SSM and apply S4D [GGGR22] to replace the original MH-EMA [MZK⁺23] kernel. The S4D variant of our model has much better training efficiency but the quality are significantly worse than SeqBoat-full with the default hyperparameter setting. It is possible that a well-tuned S4D kernel can have better performance than the MH-EMA for the use case of SMA but we leave a more comprehensive study as in future work. We also explore different differentiable approximation of latent decision making by replacing Tempered Softmax with Gumbel Softmax [JGP17]. However, we don’t observe the performance improvements over Tempered Softmax for our setting. More details of the implementation of Gumbel Softmax based latent configurator is shown in Appendix A.3.

Table 6: Ablation study on Image and ListOps of the LRA benchmark. We report the validation accuracy on the Image and ListOps tasks, together with the training speed up for each of the tasks compared with MEGA.

| Model | Image | Speed (↑) | ListOps | Speed (↑) |
|--------------------|--------------|------------------|----------------|------------------|
| SeqBoat-full | 90.16 | 1.45× | 60.95 | 1.79× |
| - Always Activated | 90.70 | 1.25× | 62.10 | 1.11× |
| - Gumbel Softmax | 89.94 | 1.29× | 59.75 | 1.76× |
| - SSM with S4D | 82.84 | 1.88× | 59.25 | 2.45× |

E Limitations & Broader Impact

The Sparse Modular Activation (SMA) and the SeqBoat architecture can bring about considerable societal impact by enhancing the efficiency and interpretability of sequence modeling tasks. These advancements can result in better-performing automated systems, like open-domain chatbot and automatic speech recognition, potentially improving communication, fostering inclusivity, and making such services more accessible to various societal sectors. The enhanced interpretability of models can generate trust in AI systems, especially in sensitive sectors like healthcare and finance. Transparent

AI models can assist professionals in these fields to make better-informed decisions, potentially leading to improved societal outcomes.

However, these improvements come with a notable limitation: our research was unable to conduct experiments on models with a large number of parameters due to computational resource constraints. As such, while the proposed mechanisms show promising results in the tested scenarios, their scalability and applicability to larger, more complex models remain uncertain. This limitation may restrict the broader applicability of our findings, especially for large-scale problems or when fine-grained control over the model's behavior is needed. Furthermore, ethical considerations such as data privacy need to be seriously considered as our work progresses. As the efficiency of these models increases, there's an increased potential for processing large amounts of personal data, which necessitates robust privacy safeguards. Future work will focus on addressing these limitations and ethical concerns, to ensure the advantages of these models can be responsibly realized.